

Electronic Supplementary Information for

Sulfonated silica/carbon nanocomposites as novel catalysts for hydrolysis of cellulose to glucose

Stijn Van de Vyver, Li Peng, Jan Geboers, Hans Schepers, Filip De Clippel, Cedric Gommès, Bart Goderis, Pierre A. Jacobs, Bert F. Sels*

Center for Surface Chemistry and Catalysis, K.U. Leuven, Kasteelpark Arenberg 23, 3001 Heverlee, Belgium. E-mail: bert.sels@biw.kuleuven.be

1 Catalyst preparation

Silica/carbon nanocomposites were synthesized by the evaporation-induced triconstituent co-assembly method, wherein sucrose is used as carbon precursor, prehydrolyzed tetraethyl orthosilicate (TEOS) as silica precursor, and Pluronic F127 triblock copolymer (EO₁₀₆PO₇₀EO₁₀₆, $M_w = 12600$) F127 as structure-directing amphiphilic surfactant. In a typical preparation, 6.4 g block copolymer F127 was dissolved in 32 g ethanol with 0.3 g concentrated HCl (37%) and the mixture was treated in an ultrasonic bath for 1 h to afford a clear solution. Next, 8.32 g TEOS and 10 g sucrose solution with different concentration were added in sequence. After being treated in an ultrasonic bath for another 1 h, the mixture was transferred into dishes. It took 20 h at 313 K to evaporate ethanol and 24 h at 433K to thermopolymerize. Carbonization was done at 673K or 823K for 15 h under N₂ flow.

Three samples with different carbon content of 66 wt%, 50 wt % and 33wt % were synthesized by changing the concentration of the sucrose solution added. These materials were treated with concentrated sulfuric acid (1 g of solid/20 ml of H₂SO₄) at 423 K for 15 h in a Teflon-lined autoclave. The resulting materials were washed with hot distilled water until no sulfate ions were detected in the wash water. The as-prepared sulfonic acid functionalized silica/carbon nanocomposites are further denoted as SimCn-T-SO₃H (m, n are the weight percentages of silica and carbon, respectively, and T is the carbonization temperature in Kelvin).

The sulfonated amorphous sugar catalyst was prepared according to the procedure reported by Toda *et al.*,¹ with some changes: sucrose, instead of D-glucose, was used as starting material and the sulfonation was carried out in a closed Teflon-lined autoclave rather than in a N₂ atmosphere. The sulfonation procedure of this amorphous sugar catalyst was performed in the same manner as described above.

2 Catalyst characterization

Characterization of the sulfonated silica/carbon nanocomposites was carried out by a combination of Thermogravimetric Analysis (TGA), Small-Angle X-ray Scattering (SAXS), N₂ physisorption and Scanning Electron Microscopy (SEM).

A Thermogravimetric analysis

The carbon content in the sulfonated silica/carbon nanocomposites was measured by Thermogravimetric Analysis (TGA) in O₂, as shown in Figure S1. TGA was performed on a TGA Q500 (TA Instruments, Brussels, Belgium). The samples were heated from room temperature to 800 °C at 5 °C min⁻¹. For the sulfonic acid group-functionalized carbon-silica composite, the weight loss below 100 °C and in range of 100–600 °C in O₂ can be attributed to the absorbed water and carbon compound, respectively, while the weight residue belongs to the silica.

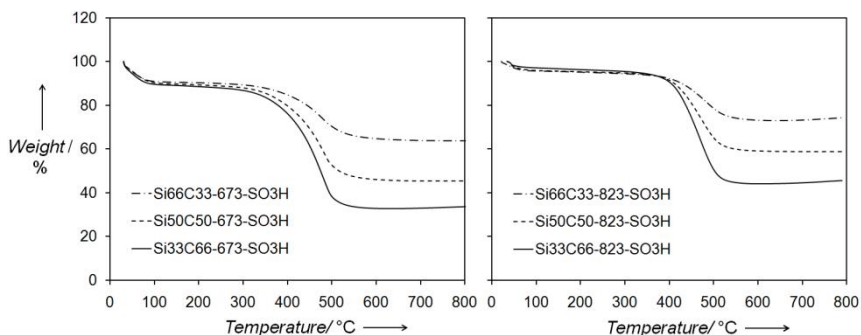


Fig. S1 TGA curves of samples Si33C66-673-SO₃H, Si50C50-673-SO₃H, Si66C33-673-SO₃H, Si33C66-823-SO₃H, Si50C50-823-SO₃H and Si66C33-823-SO₃H.

B Small-Angle X-ray Scattering

The SAXS patterns of all samples were measured at the Dutch-Belgian beamline (BM26) of the European Synchrotron Radiation Facility² and a custom software was used to reduce the measured 2D data into 1D scattering patterns.³ Average distances between neighboring pores in Table S1 were calculated as $a = 4\pi/(\sqrt{3}q^*)$, where q^* is the scattering vector of the first peak (see Figure 1 in the manuscript).

Table S1 Average distance between neighboring pores from Small-Angle X-ray Scattering patterns.

Entry	Sample	a / nm	Δ_a / nm ^a
1	Si33C66	17.2	—
2	Si50C50	15.5	—
3	Si66C33	13.9	—
4	Si33C66-673	13.6	3.6
5	Si50C50-673	12.7	2.8
6	Si66C33-673	12.7	1.2
7	Si33C66-823	12.8	4.4
8	Si50C50-823	11.9	3.6
9	Si66C33-823	11.9	2.0

^a Δ_a is the average shrinkage between neighboring pores after carbonization of the nanocomposites.

C Nitrogen physisorption

Nitrogen adsorption/desorption isotherms in Figure S2 and Figure S3 were recorded with a Micromeritics Tristar 3000 apparatus at 77 K. Prior to physisorption measurements, the catalyst samples were evacuated at 393 K for 10 h. The surface area (S_{BET}) in Table 2 in the manuscript was deduced from the BET equation in the 0.05–0.3 relative pressure range. The total pore volume (V_{tot}) is calculated from the saturation plateau at high relative pressure by assuming that N_2 is in the liquid state. Mesopore volume (V_{meso}) was determined according to the t-plot method. Finally, average mesopore diameters (D_{meso}) were calculated from adsorption branches of the isotherms, based on the Brunauer–Joyner–Halenda method.

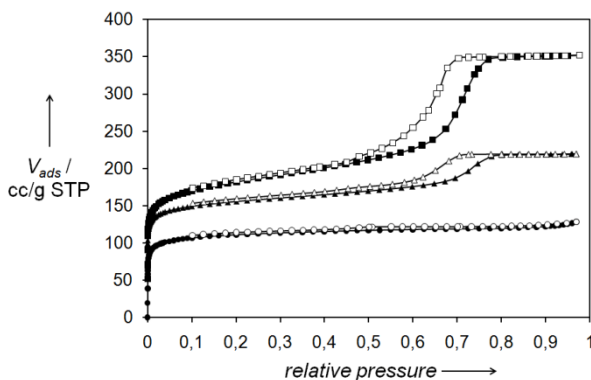


Fig. S2 N_2 adsorption/desorption isotherms of samples Si33C66-673- SO_3H (circles), Si50C50-673- SO_3H (triangles) and Si66C33-673- SO_3H (squares). For clarity, the isotherms of Si50C50-673- SO_3H and Si66C33-673- SO_3H are offset along the Y axis by $50 \text{ cm}^3 \text{ g}^{-1}$.

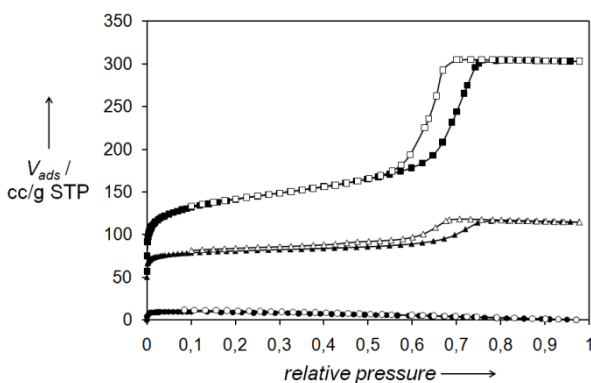


Fig. S3 N_2 adsorption/desorption isotherms of samples Si33C66-823- SO_3H (circles), Si50C50-823- SO_3H (triangles) and Si66C33-823- SO_3H (squares). For clarity, the isotherms of Si50C50-823- SO_3H and Si66C33-823- SO_3H are offset along the Y axis by $50 \text{ cm}^3 \text{ g}^{-1}$.

D Scanning Electron Microscopy

The as-prepared silica/carbon nanocomposites were further examined with a high resolution Scanning Electron Microscope (Philips XL-30 FEG). Representative micrographs of the Si33C66-550-SO₃H sample are shown in Figure S4.

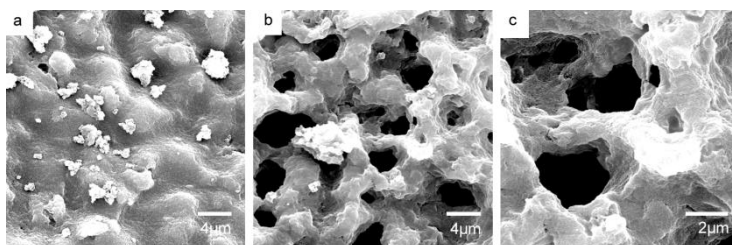


Fig. S4 SEM micrographs of the Si33C66-550-SO₃H catalyst system.

3 Zeolite properties

Table S2 Properties and origin of zeolite samples used.

Entry	Product name	Framework type	Bulk Si/Al ratio	Al _{Framework} ^a / %	Specific surface/ m ² g ⁻¹	Manufacturer
1	ZM 510	MOR	11	84	510	Zéocat
2	CP 811-25	BEA	9.9	76	730	Süd-Chemie
3	H-ZSM 5	MFI	40	95	n.d. ^b	Süd-Chemie
4	CBV 400	FAU	2.6	n.d. ^b	730	PQ zeolites
5	CBV 600	FAU	2.6	27	660	PQ zeolites
6	CBV 720	FAU	15	68	780	PQ zeolites
7	CBV 760	FAU	25	99	720	PQ zeolites
8	CBV 780	FAU	40	99	780	PQ zeolites
9	CBV 901	FAU	42	99	700	PQ zeolites

^a% of framework Al as measured by ²⁹Si NMR in the case of FAU or by ²⁷Al NMR in the case of H-ZSM-5 and H-Beta.⁴⁻⁶ ^bn.d.: not determined.

4 Cellulose pretreatment and characterization

Cellulose (Avicel PH-101, microcrystalline) was characterized (i) as received from Sigma-Aldrich and (ii) after 24 h ball-milling pretreatment. Ball-milling with 25 g of cellulose was carried out using ZrO₂ balls (mass 7.5 g; diameter 1.8 cm). SEM images of cellulose before and after ball-milling are given in Figure S5.

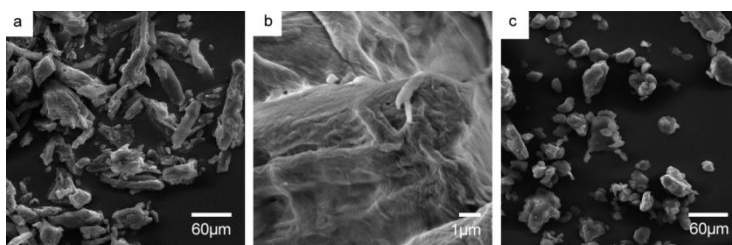


Fig. S5 SEM characterization of cellulose before (a-b) and after ball-milling (c).

X-ray diffraction (XRD) patterns of the Ni/CNF catalyst were recorded at room temperature with a STOE STADI P Combi diffractometer. The diffracted intensity of CuK α radiation (wavelength of 0.154 nm) was measured in a 2θ range between 0° and 75° . Figure S6 displays XRD patterns taken of cellulose samples unmilled and ball-milled for 24 h. In the untreated cellulose, the major peak at $2\theta = 22.5^\circ$ can be assigned to the crystalline plane 002. A comparison of the patterns clearly reveals a decrease in crystallinity of the cellulose feedstock after ball-milling pretreatment.

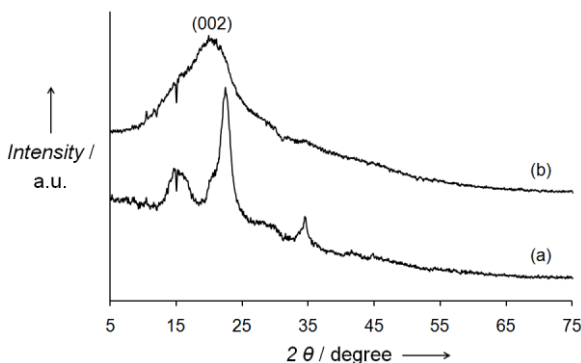


Fig. S6 Powder X-ray diffraction patterns of cellulose before (a) and after ball-milling (b).

The ^{13}C CP MAS NMR spectra of cellulose with and without ball-milling were recorded on a Bruker Avance DSX400 spectrometer (9.4 T). 4400 scans were accumulated with a recycle delay of 10 s. The contact time was 4 ms. The samples were packed in 4 mm rotors, and the spinning frequency of the rotor was 5000 Hz. Tetramethylsilane was used as shift reference. The decreasing peak ratios of $\text{C4}_{(86-92 \text{ ppm})}/\text{C4}_{(79-86 \text{ ppm})}$ and $\text{C6}_{(63-67 \text{ ppm})}/\text{C6}_{(56-63 \text{ ppm})}$ in Figure S7 are in good agreement with the reported literature observations.⁷ This, in interplay with the above XRD data, strongly suggests that more disordered cellulose is produced after the mechanical ball-milling treatment. Furthermore, line widths are larger in the amorphous sample which is due to the large distribution of molecular orientations.

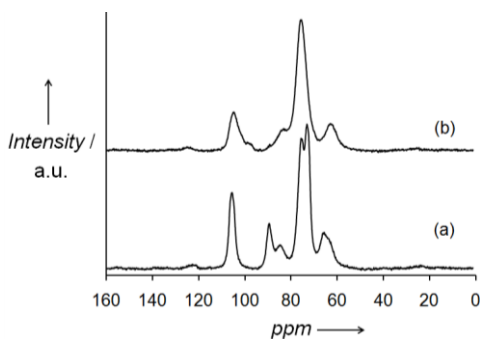


Fig. S7 ^{13}C CP MAS NMR spectra of cellulose before (a) and after ball-milling (b).

IR spectra were recorded under vacuum from KBr pellets on a Bruker IFS 66v/S instrument. The spectra in Figure S8 also show the changes in the cellulose structure after ball-milling. The less pronounced band at 1430 cm^{-1} is another strong indication of a less ordered cellulose sample, since it is assigned to the CH_2 scissoring motion in the cellulose I crystal. The ball-milling allows the regular arrangement of the CH_2OH group on C_6 to relax into a more random one, resulting in a broader band at 1430 cm^{-1} .

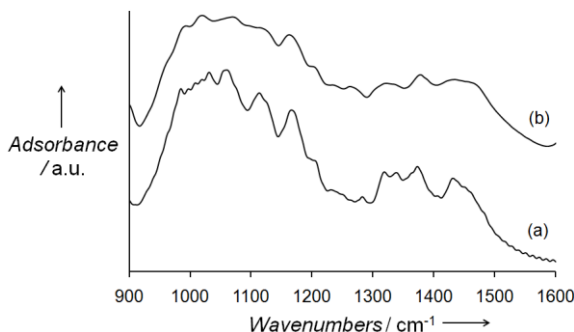


Fig. S8 IR spectra of cellulose before (a) and after ball-milling (b).

5 Catalytic hydrolysis reactions of cellulose

Catalysts (50 mg), cellulose (Avicel PH-101, 50 mg) pretreated by mechanical ball-milling and distilled water (5 ml) were loaded into a teflon-lined stainless steel reactor (25 mL) under air. The reactor was heated at 423 K for 24 h with vigorous stirring. After reaction, the product mixture was centrifuged, filtered over a $0.45\text{ }\mu\text{m}$ PTFE filter and analyzed by HPLC (Agilent 1200 Series, Varian Metacarb 67C column ($300 \times 6.5\text{ mm}$), mobile phase: water), equipped with an RI detector. Figure S9 shows chromatograms of the liquid recovered from a blank experiment and catalytic reactions with solid acids Amberlyst 15 and Si33C66-823- SO_3H .

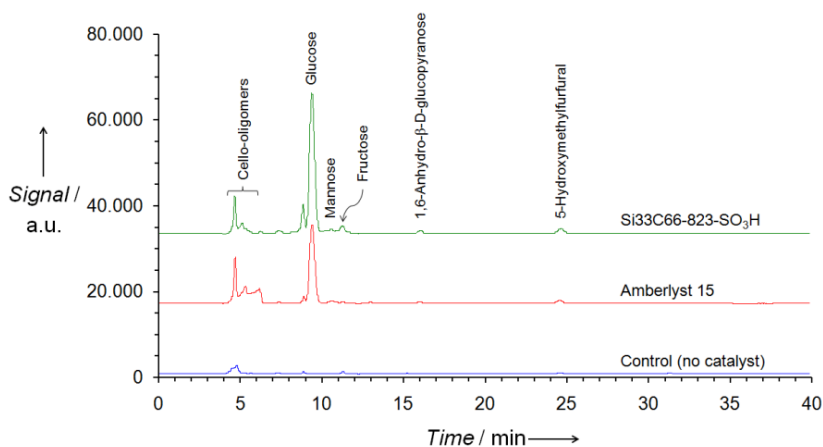


Fig. S9 Chromatograms of cellulose conversion over Amberlyst 15, Si33C66-823- SO_3H and the blank reaction without catalyst.

The assigned compounds were identified by comparison of retention times with those of the corresponding reference compounds. Conversions of cellulose were determined by total organic carbon (TOC) analysis of the liquid phase, as reported earlier.⁸ Catalyst system Si33C66-823-SO₃H was studied in detail by following the kinetics of glucose formation during the reaction (Figure S10).

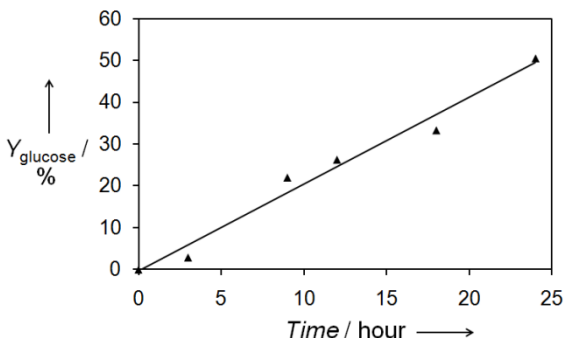


Fig. S10 Yields to glucose for the hydrolytic conversion of cellulose catalyzed by Si33C66-823-SO₃H as a function of reaction time.

References

- 1 M. Toda, A. Takagaki, M. Okamura, J. N. Kondo, S. Hayashi, K. Domen and M. Hara, *Nature*, 2005, **438**, 178.
- 2 W. Bras, I. P. Dolbnya, D. Detollenaere, R. van Tol, M. Malfois, G. N. Greaves, A. J. Ryan and E. Heeley, *J. Appl. Crystallogr.*, 2003, **36**, 791.
- 3 C. J. Gommers and B. Goderis, *J. Appl. Crystallogr.*, 2010, **43**, 352.
- 4 P. P. Pescarmona, K. P. F. Janssen, C. Delaet, C. Stroobants, K. Houthoofd, A. Philippaerts, C. De Jonghe, J. S. Paul, P. A. Jacobs, B. F. Sels, *Green Chem.*, 2010, DOI: 10.1039/b921284a.
- 5 J. M. Thomas, *J. Mol. Catal.*, 1984, **27**, 59.
- 6 A. Omegna, J. A. van Bokhoven and R. Prins, *J. Phys. Chem. B*, 2003, **107**, 8854.
- 7 H. Zhao, J. H. Kwak, Y. Wang, J. A. Franz, J. M. White and J. E. Holladay, *Energy Fuels*, 2006, **20**, 807.
- 8 N. Ji, T. Zhang, M. Zheng, A. Wang, H. Wang, X. Wang, Y. Shu, A. L. Stottlemyer and J. G. Chen, *Catal. Today*, 2009, **147**, 77.